NEUROIMAGE 2, 45–53 (1995)

Analysis of fMRI Time-Series Revisited

K. J. FRISTON, A. P. HOLMES, J-B. POLINE, P. J. GRASBY, S. C. R. WILLIAMS,† R. S. J. FRACKOWIAK, AND R. TURNER

The Wellcome Department of Cognitive Neurology, Institute of Neurology, Queen Square WC1N 3BG, United Kingdom; the MRC Cyclotron Unit, London W12 OHS, United Kingdom; and †The Institute of Psychiatry, Denmark Hill, London SE5 8AZ, United Kingdom

Received February 14, 1995

This paper presents a general approach to the analysis of functional MRI time-series from one or more subjects. The approach is predicated on an extension of the general linear model that allows for correlations between error terms due to physiological noise or correlations that ensue after temporal smoothing. This extension uses the *effective degrees of freedom* associated with the error term. The effective degrees of freedom are a simple function of the number of scans and the temporal autocorrelation function. A specific form for the latter can be assumed if the data are smoothed, in time, to accentuate hemodynamic responses with a neural basis. This assumption leads to an expedient implementation of a flexible statistical framework. The importance of this small extension is that, in contradistinction to our previous approach, any parametric statistical analysis can be implemented. We demonstrate this point using a multiple regression analysis that tests for effects of interest (activations due to word generation), while taking explicit account of some obvious confounds.

INTRODUCTION

In a previous communication we considered the effect of temporal correlations on making statistical inferences about the relationship between a reference waveform and time-series obtained with "fast" MRI techniques (e.g., EPI). In this paper we present a more comprehensive approach to dealing with these correlations, which is based on the general linear model and a heuristic analysis of the "effective degrees of freedom."

fMRI time-series contain a number of signals; these include uncorrelated noise (e.g., Quantum noise and thermal noise), correlated noise (e.g., physiological noise from cardiac and respiratory cycles), and a correlated signal that conforms approximately to changes in neural activity convolved with a hemodynamic response function (Friston *et al.,* 1994a). Correlated noise can arise directly from cardiac and respiratory cycles, their physiological modulation (e.g., the heart rate variability signal), or aliasing of these effects due to an interaction with the repeat time. Convolution of the fMRI time-series with the hemodynamic response function will, in principle, enhance signal relative to noise, particularly thermal and other noise with high frequency components. However, low frequency physiological noise and temporal smoothing render scans correlated in time. This violates a fundamental assumption of the general linear model, which assumes each scan is an independent observation. The aim of this work was to extend the general linear model so that it could be applied to data with a stationary and known autocorrelation among the observations and thereby facilitate the analysis of temporally smoothed data.

Temporal Autocorrelations and Smoothing

It is important to be clear about the pretext for the approach advocated in this paper. One of its main tenets is that a more powerful test obtains if the data are smoothed in time. This denoising device is based on the conjecture that "interesting" hemodynamics are the result of convolving an underlying neuronal process with a hemodynamic response function. As such the signal is always "smoother" than (or as smooth as) the response function. This conjecture is based on our previous analyses of fMRI time-series (Friston *et al.,* 1994a) and some compelling and convergent empirical results (e.g., Bandettini *et al.,* 1993). More specifically we assume that a fMRI time-series has a number of linearly separable [variance] components that include high frequency noise, low frequency noise, and low frequency signal. The relative amounts of these components will change with field strength, pulse sequence, and experimental design; however, given that all these components exist, smoothing will always increase signal to noise. Clearly the optimum smoothing kernel is related to the hemodynamic response function. "Optimum" refers to the kernel that maximizes variance in the signal frequencies relative to other frequencies. Our previous

1053-8119/95 $6.00

analysis, and review of the literature, suggested that the hemodynamic response function has an associated delay and dispersion of about 6–8 s. This corresponds to a Gaussian kernel of width $\sqrt{6} = 2.45$ to $\sqrt{8} = 2.83$ s. The value adopted for temporal smoothing in this paper is 2.83 s. In Friston *et al.* (1994a) we assumed a Poisson form for the response function and noted that this is roughly the same as a Gaussian form at the degrees of dispersion seen in fMRI.

In summary, based on the above assumptions, one concludes that it is always better to smooth the data, in time, to increase hemodynamic variance components with a neuronal basis, relative to other components. It may be thought that the reduction in the effective degrees of freedom that ensues could reduce statistical power. However, the increased degrees of freedom observed in unsmoothed data derive from uncorrelated variance components that are almost certainly noise and, in general, adding noise to an observed response variable does not increase power. It should be pointed out that these arguments may have to be revised with advances in fMRI pulse sequences and an increased understanding of the relationship between neuronal dynamics and hemodynamics, but at present they represent a reasonable and consistent set of assumptions.

In this paper we make the simplifying assumption that, after temporal smoothing, the correlations that manifest are stationary and (almost) completely accounted for by the convolution (or smoothing operation). Clearly this is wrong if there are substantial low frequency physiological components in the original data. However, in raw data, physiological components are often small relative to uncorrelated components (e.g., thermal noise, digitizing noise, or quantal effects). Furthermore the difference between the assumed correlations and those observed will be small even if physiological noise dominates. For example, consider a component due to physiological effects that could be emulated by convolving white noise with a Gaussian kernel of parameter (i.e., standard deviation) 1 s. Smoothing with a Gaussian kernel of parameter 3 s would render the correlation length (standard deviation of the autocorrelation function) of this component $\sqrt{\{2(1^2 + 3^2)\}} = 4.47$ s. The correlation length due to the convolution alone, or equivalently any uncorrelated components after convolution, is $3\sqrt{2} = 4.24$ s. The disparity is not great.

This paper is divided into two parts. The first part presents the theory and provides operational equations. The theory section reviews the general linear model and considers the incorporation of temporal smoothing. The effect of smoothing is modeled in terms of identically distributed error terms with a known stationary covariance structure. This form for the error terms leads to an expression for the effective degrees of freedom that is used to compute the t statistic testing for a linear compound of effects (e.g., activation effects, time effects, subject or block effects, and so on). These sections conclude with a brief review of results developed in statistical parametric mapping. These results are required to make statistical inferences about the regional effects in the resulting SPM{t}. The second half presents a validation and application of the theoretical results using fMRI data obtained during a series of word generation tasks.

THEORY

All parametric statistics are based on the general linear model (Chatfield and Collins, 1980). In the context of functional imaging the general linear model is used to make statistical inferences by performing univariate tests at each and every voxel. This is known as statistical parametric mapping. The nature of the hypothesis, or inference sought, can be very diverse. In what follows we present a framework that can accommodate any form of parametric statistical test ranging from correlation with a single reference vector, in a single subject design, to mixed multiple regression/ANCOVA models in many subjects. This general approach has been described in detail elsewhere but will be summarized for completeness in this paper. The extensions to the general linear model considered in this paper concern temporal smoothing and the effect that this has on the effective degrees of freedom associated with the error terms.

The General Linear Model

The general linear model for a time-series can be written in matrix notation as

$$\begin{aligned}\mathbf{X} &= \mathbf{H} \cdot \eta + \mathbf{D} \cdot \gamma + \mathbf{e} \\ &= \mathbf{G} \cdot \beta + \mathbf{e}, \end{aligned} \tag{1}$$

where $\mathbf{X}$ is a column vector of response variables, in this case, mean corrected values from a single voxel in a fMRI time-series. The columns of $\mathbf{H}$ model the effects of interest, for example, one or more reference waveforms or vectors, performance, or some psychophysical score. The columns of $\mathbf{D}$ model effects of no interest that are considered confounds, for example, time, a subject-specific effect, or the global activity, the scan. $\mathbf{H}$ and $\mathbf{D}$ are partitions of the design matrix $\mathbf{G} = [\mathbf{H}\ \mathbf{D}]$. The design matrix has one row for every scan and one column for every effect (factor or covariate) in the model. The columns of the design matrix can be covariates (e.g., "time on target" or global activity) or can be "indicator" variables that take the value 0 or 1, depending on whether a specific effect is present or not (e.g., the data come from the third subject or were obtained under the condition "A"). Note that there is no mathe-

matical distinction between covariates and indicator type variables. $\boldsymbol{\beta} = [\eta^T\ \gamma^T]^T$ is a column vector of parameters for the "effects" modeled by each column of the design matrix. The errors **e** are assumed to be independent and identically normally distributed with covariance $\Sigma = \sigma^2 \cdot \mathbf{1}$, where **1** is the identity matrix.

The general linear model can now be extended to include temporal smoothing. Let **K** be a convolution matrix using a Gaussian kernel with parameter s, where, by Eq. (1)

$$\mathbf{K} \cdot \mathbf{X} = \mathbf{G}^* \boldsymbol{\beta} + \mathbf{K} \cdot \mathbf{e}, \tag{2}$$

where $\mathbf{K} \cdot \mathbf{X}$ represents temporally smoothed data. $\mathbf{G}^* = \mathbf{K} \cdot \mathbf{G}$ is a similarly convolved design matrix **G,** whose columns may include a suitably delayed box-car reference vector convolved with **K,** and **K** is chosen to emulate the dispersion associated with the hemodynamic response function. At first glance it may seem odd to convolve all the columns of the design matrix **G** especially those containing indicator type variables or covariates with no special relationship to "smooth" hemodynamics (e.g., global activity). However, it should be remembered that the effect in $\mathbf{K} \cdot \mathbf{X}$, modeled by every column of **G,** is smoothed or distributed in time and it is therefore necessary to smooth the corresponding explanatory variable in **G** to give $\mathbf{G}^*$.

In this convolved version of the general linear model [Eq. (2)] the error terms are identically distributed with covariance $\Sigma = \sigma^2 \cdot \mathbf{K} \cdot \mathbf{K}^T$. Least-squares estimates of $\boldsymbol{\beta}$, say $\mathbf{b} = [\mathbf{h}^T\ \mathbf{g}^T]^T$, are given by

$$\mathbf{b} = (\mathbf{G}^{*T}\mathbf{G}^*)^{-1}\mathbf{G}^{*T} \cdot \mathbf{K} \cdot \mathbf{X},$$

where

$$\mathrm{E}\{\mathbf{b}\} = \beta \text{ and } \mathrm{Var}\{\mathbf{b}\} = \sigma^2(\mathbf{G}^{*T}\mathbf{G}^*)^{-1}. \tag{3}$$

Var{**b**} is the variance–covariance matrix for the parameter estimates. After estimating $\boldsymbol{\beta}$, the adjusted smoothed data $\mathbf{X}^*$ are given by discounting the effects of no interest estimated by **g** (e.g., time effects, subject, or more generally block effects):

$$\mathbf{X}^* = \mathbf{K} \cdot (\mathbf{X} - \mathbf{D} \cdot \mathbf{g}) \tag{4}$$

and are sometimes a useful form in which to report the data.

Testing a Hypothesis

In this section we address statistical inferences about the effects of interest (e.g., the significance of the regression coefficient for a reference waveform in **H**). The null hypothesis that the effects embodied in **H** are not significant can be tested with the t statistic using linear compounds or contrasts of the parameter estimates **b.** A contrast (row vector) **c** is simply a set of weights that sum to zero. We present the more general test for linear compounds of the effects and note that if there is only one effect, $\mathbf{c} = 1$. The significance of a particular linear compound of effects is tested with

$$T = \mathbf{c} \cdot \mathbf{b}/(\mathbf{c} \cdot \epsilon^2 \cdot (\mathbf{G}^{*T}\mathbf{G}^*)^{-1} \cdot \mathbf{c}^T)^{1/2}, \tag{5}$$

where, from Eq. (3) $\mathrm{Var}(\mathbf{c} \cdot \mathbf{b}) = \mathbf{c} \cdot \sigma^2 \cdot (\mathbf{G}^{*T}\mathbf{G}^*)^{-1} \cdot \mathbf{c}^T$ ϵ^2 is the estimate of σ^2 and is based on the residual or error terms **r** obtained from the difference between the actual and the estimated values of $\mathbf{K} \cdot \mathbf{X}$**:**

$$\mathbf{r} = \mathbf{K} \cdot \mathbf{X} - \mathbf{G}^* \cdot \mathbf{b},$$

where

$$\epsilon^2 = \mathbf{r}^T \cdot \mathbf{r}/\nu. \tag{6}$$

ν is the degrees of freedom associated with **r,** and T has the Students t distribution with degrees of freedom ν. If the error terms (elements of **r**) were independently distributed, ν would simply be the number of scans (N) minus the number of effects estimated, i.e., N − rank($\mathbf{G}^*$). However, the error terms are known to be correlated because of the temporal smoothing ($\Sigma = \sigma^2 \cdot \mathbf{K} \cdot \mathbf{K}^T$). This brings us to the extension of the general linear model that uses an expression for ν in terms of N, rank($\mathbf{G}^*$) and the kernel in the convolution matrix **K.**

The Effective Degrees of Freedom

In this section we consider the effective degrees of freedom of the error terms using a simple analysis in the frequency domain. Following Worsley *et al.* (in preparation) we shall argue that the sum of squares due to error $S = \mathbf{r}^T \cdot \mathbf{r} = \mathbf{r}'^T \cdot \mathbf{r}'$ has a scaled χ^2 distribution, where $\mathbf{r}'$ is considered to be a [N − rank($\mathbf{G}^*$)]-variate random vector with the same covariance as **r;** i.e., $\mathbf{r}'$ is the projection of the original error vector **r** onto a [N − rank($\mathbf{G}^*$)] dimensional subspace. This projection corresponds to the removal of rank($\mathbf{G}^*$) dimensions from the original data that represent the effects modeled in $\mathbf{G}^*$. Using this conjecture the effective degrees of freedom are simply determined using the known moments (mean and variance) of S over many realizations of $\mathbf{r}'$. Let $g(\omega_i)$ be the spectral density of the process $\mathbf{r}'$ following a discrete Fourier transform, where $\omega_i = 2\pi i/[N - \mathrm{rank}(\mathbf{G}^*)]$. The expectation or mean of S is simply the sum of the expectations of all N − rank($\mathbf{G}^*$) components at each frequency ω_i.

$$E\{S\} = \Sigma\, g(\omega_i). \tag{7}$$

By independence the variance of S is the sum of the variances of each component at ω_i. Every component has a χ^2 distribution with 1 degree of freedom, scaled by $\{g(\omega_i)\}^{-1}$, and the variance of a χ^2 distribution with 1 degree of freedom is 2. Therefore the variance of each component is simply $2 \cdot \{g(\omega_i)\}^2$ and the total variance is

$$\mathrm{Var}\{S\} = \Sigma\, 2 \cdot \{g(\omega_i)\}^2. \tag{8}$$

Let the distribution of S be given by $\chi^2\nu(s/a)$ with ν degrees of freedom. a is the scaling of the required χ^2 distribution, where

$$E\{S\} = E\{\chi^2\nu(s/a)\} = a \cdot \upsilon$$

and

$$\mathrm{Var}\{S\} = \mathrm{Var}\{\chi^2\nu(s/a)\} = 2 \cdot a^2 \cdot \nu.$$

Solving for ν, using Eqs. (7) and (8)

$$\nu = \Sigma\, g(\omega_i) \cdot \Sigma\, g(\omega_i)/\Sigma\, \{g(\omega_i)\}^2. \tag{9}$$

Equation (9) gives a general expression for the effective degrees of freedom for any arbitrary frequency structure or temporal smoothing in the error (and other) terms. In the case considered here the smoothing is Gaussian with parameter s, where $\Sigma = \sigma^2 \cdot \mathbf{K} \cdot \mathbf{K}^T$ and the autocovariance function and spectral density are

$$\rho(i) = \sigma^2 \cdot \exp(-i^2/4s^2)$$

$$g(\omega_i) = 2 \cdot \sigma^2 \cdot s \cdot \pi^{1/2} \cdot \exp(\omega_i^2 \cdot s^2)$$

giving

$$\nu = [N - \mathrm{rank}(\mathbf{G}^*)]/\sqrt{(2\pi s^2)}. \tag{10}$$

Note that the effective degrees of freedom scale up with increased number of scans (N) and down with the smoothness (s) and the number of effects modeled [rank($\mathbf{G}^*$)]. By using the above expressions [Eqs. (5), (6), and (10)] we obtain a value for T at each and every voxel. These constitute a statistical parametric map or SPM$\{t\}$. To simplify subsequent analysis, the SPM$\{t\}$ is transformed to a SPM$\{Z\}$ using a probability integral transform or other standard device.

Relationship to Our Previous Work

In Friston *et al.* (1994a) we considered the limited case of correlating a reference waveform with a fMRI time-series and addressed the problem of how to estimate the effective degrees of freedom associated with this correlation. Here we present a framework that is completely general and is designed to facilitate parametric tests of almost any nature. In the foregoing paper we presented an analysis in continuous time to argue that effective degrees of freedom associated with the sum of products of two processes x and y, with spectral densities $g_x(\omega)$, and $g_y(\omega)$ is given by

$$\nu = \int g_x(\omega)d\omega \int g_y(\omega)\, d\omega / \int g_x(\omega)\, g_y(\omega)\, d\omega. \tag{11}$$

In this paper we consider the effective degrees of freedom associated with the sum of squares of the error terms. By representing the error terms as $x = y$, where $g_x(\omega) = g_y(\omega)$ the formal equivalence between Eq. (9) and Eq. (11) becomes obvious.

Statistical Inference

In this section we consider the interpretation of the SPM$\{Z\}$ in terms of probability levels or p values. The problem here is that an extremely large number of non-independent univariate comparisons have been performed and the probability that any region of the SPM will exceed an uncorrected threshold by chance is high. Standard procedures have been developed in statistical parametric mapping that correct for the multiplicity of voxels and the spatial correlations among them. These corrections are based on either the height (Z) or the spatial extent (n) of a local excursion of the SPM (i.e., cluster of voxels above a threshold). The distributional approximations required for these corrections derive from the theory of Gaussian random fields and will not be reviewed in detail here [see Friston *et al.*, 1991; Worsley *et al.*, 1992; and Friston *et al.*, 1994b, for the development of this theory in functional imaging and Adler, 1981, for a comprehensive discussion of the underlying theory. Some newer technical results can be found in Worsley, 1994]. The main results are:

- The probability of getting at least one voxel with a Z value of height u or more, in a D dimensional SPM$\{Z\}$ of volume V is the same as the probability that the largest Z value in the entire volume (Z_{max}) is greater than u, where

$$P(Z_{max} > u) \leq E\{m\} \approx V \cdot (2\pi)^{-(D+1)/2}\, W^{-D}\, u^{D-1} \exp(-u^2/2), \tag{12}$$

and $E\{m\}$ is the expected number of maxima. W is a measure of spatial smoothness and is related to the full width at half maximum (FWHM) of the SPM. In practice W can be determined directly from the effective FWHM if it is known, when $W = \mathrm{FWHM}/\sqrt{4\ln 2)}$ or estimated post hoc using the measured variance of the SPM's first partial derivatives. See Friston *et al.* (1991) and Worsley *et al.* (1992) for more details.

• The probability of getting one or more regions of size k or more in a given SPM{Z} of volume V, thresholded at t, is the same as the probability that the largest region (n_{max}) consists of k or more voxels where

$$P(n_{max} \geq k) = 1 - \exp[-E\{m\} \cdot \exp(-\beta k^{2/D})]$$

and

$$\beta = [\Gamma(D/2 + 1) \cdot E\{m\}/V \cdot \Phi(-t)]^{2/D}. \quad (13)$$

$\phi(-\dagger)$ is the integral of the unit Gaussian distribution evaluated at the threshold chosen ($-t$). Equation (13) gives an estimate of the probability of finding at least one region with k or more voxels in an SPM{Z}.

In this paper we present P values that are based on both the spatial extent and the peak height. The uncorrected P values are simply $\phi(-t)$. Note that neither of the above expressions for P values specify what threshold to use. For high resolution, fMRI lower thresholds (e.g., 2.8) may be more powerful (see Friston *et al.*, 1994b).

APPLICATION TO EMPIRICAL DATA AND VALIDATION

In these sections we describe the experimental design and data used to illustrate the application of the above theory. In particular we focus on validation by assessing the distribution of voxel values under the null hypothesis. In order to assess the validity of our simplifying assumptions we used *real* data but a totally *random* design matrix partition **H.** Because the effects of interest are random, the null hypothesis (that the effects modeled by **H** are negligible) is almost certainly true and the ensuing distribution of Z values should conform to the unit normal distribution.

Data Acquisition and Experimental Design

One hundred T_2* weighted volume images (128 × 64 × 10 voxels) were obtained from a single male subject using a GE/ANMR 1.5T system with EPI capabilities. The volumes consisted of 10 sequential transverse sections and were acquired every 3 s. Voxel size was 3 × 3 × 7-mm voxels with 0.5-mm slice separation. The

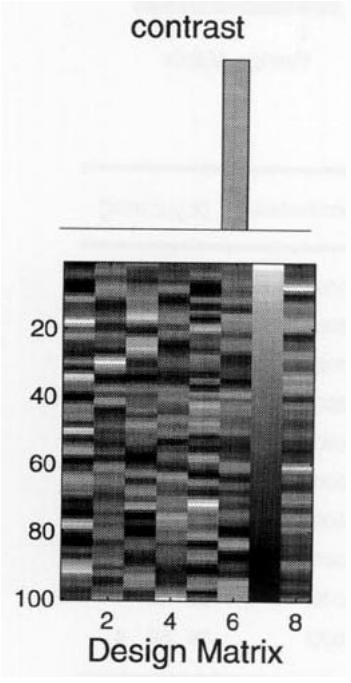

FIG. 1. Design matrix and an example of one of the six contrasts used in the validation analysis. (Top) A contrast **c** = [0 0 0 0 0 1 0 0] testing for the significance of the effect modeled in the sixth column of the design matrix. (Bottom) The design matrix **G** with six random covariates or waveforms on the left and two confounds on the right. These two confounding covariates correspond to a time effect and to global or whole volume activity. Because elements of this matrix can take negative values the gray scale is arbitrary and has been scaled to the minimum and maximum. The form of the design matrix is the same as in the text—**K** · [**H D**]. Note that the length of the contrast is the same as the number of columns, or effects, in the design matrix, which is the same as the number of parameters one is explicitly estimating.

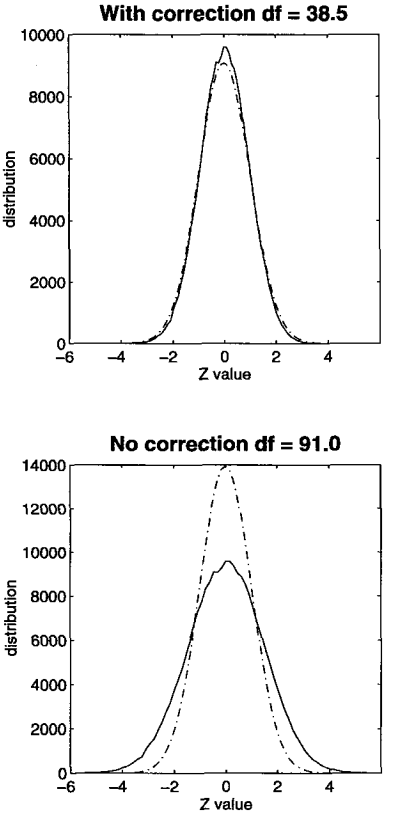

FIG. 2. Analysis of the Z distribution obtained under the null hypothesis. Z values were pooled over the six SPM{Z} derived using the design matrix in Fig. 1. The resulting distributions are shown (top) using the effective degrees of freedom (calculated as described in the main text) and (bottom) using the conventional degrees of freedom that would ensue if the error terms were assumed to be independent.

subject was scanned under two silent word generation conditions. The baseline (repeating internally a heard word) and activation (generating a word that began with a heard letter) conditions were presented in blocks of 10 scans, with 10 baseline, 10 activation, 10 baseline, and so on. The tasks were paced at one word every 3 s.

Data Prepossessing

The 100 volume images were realigned to the first as described elsewhere (Friston *et al.*, submitted) and resampled down to 2 × 2 × 4-mm voxels. The data were then smoothed with an isotropic Gaussian kernel with FWHM of 4 mm. This spatial smoothing was imple-

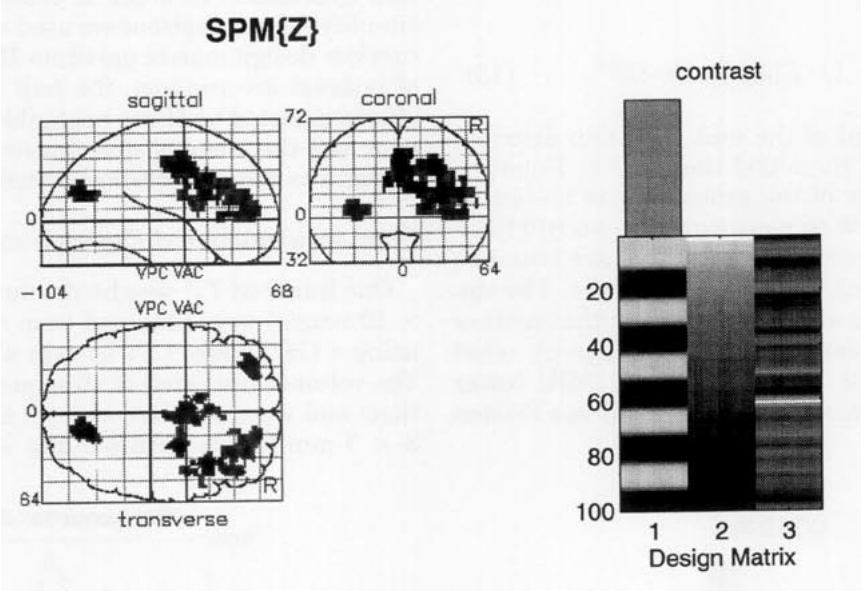

Activations

region	size {k}	P(n max > k)	Z	P(Z max > u)	(Uncorrected)	{x,y,z mm}
1	**440**	**0.000**	**4.67**	**0.048**	(0.000)	**0 −4 44**
			4.60	0.064	(0.000)	22 −8 40
			3.85	1.059	(0.000)	0 14 28
2	**138**	**0.021**	**4.59**	**0.066**	(0.000)	**14 −72 20**
			3.81	1.242	(0.000)	6 −76 24
3	**533**	**0.000**	**4.18**	**0.341**	(0.000)	**18 50 8**
			3.97	0.710	(0.000)	30 32 16
			3.90	0.909	(0.000)	36 12 20
4	**106**	**0.071**	**4.04**	**0.567**	(0.000)	**−36 46 4**
			3.43	3.947	(0.000)	−26 50 4

Threshold = 2.33; Volume [S] = 37912 voxels; df = 41

FWHM = [8.3 8.1 8.9] *mm (i.e. 1027 RESELS)*

FIG. 3. Results of the test for activations due to word generation. (Top right) This is an image representation of the design matrix **G**. (Contrast) This is the contrast or vector defining the linear compound of parameters tested (**c** = [1 0 0]). The contrast is displayed over the column of **G** that corresponds to the (activation) effect in question. (Top left) SPM{*Z*}: This is a maximum intensity projection of the SPM{*t*} following transformation to the *Z* score. The display format is standard and provides three views of the brain from the front, below, and the left-hand side. Data are presented only for regions with $P < 0.1$ corrected. The grayscale is arbitrary and the space conforms to that described in the atlas of Talairach and Tournoux (1988). (Bottom) Tabular data are presented for "significant" regions ($P < 0.1$ corrected). The location of the maximal voxel in each region is given (positive x is left) with the size of the region (k) and up to three Z maxima. For each maxima the significance is assessed in terms of $E\{m\} > P(Z_{max} > u)$ using Eq.(12) and $P(n_{max} > k)$ using Eq.(13). In this figure there are three significant regions at $P < 0.05$ that are described in the text.

mented to increase signal to noise and represents a compromise between sensitivity and spatial resolution. It should be noted that this step is not a prerequisite for the application of the theory of Gaussian fields. The "Gaussian" in Gaussian fields refers to the multivariate distribution of the voxel values, *not* the shape of the autocorrelation function (which can have any shape as long as it is continuous at zero lag).

Voxels that had values greater than 0.8 of the volume mean in all the images were selected to restrict the analysis to intracranial regions. The 37912 columns of the resulting mean corrected data matrix corresponds to **X** in the theory sections.

Data Analysis—Validation

A volume SPM{Z} was constructed using Eqs. (3), (5), (6), and (10) and a [100 × 6] design matrix partition **H** of Gaussian random variables. We treated time and global activity as confounding covariates to form **D.** Figure 1 depicts the complete design matrix **G** with the six random effects on the left and the two confounding effects on the right. The first confound was a linear time effect (a mean corrected vector running from one to 100) and the second was mean corrected global or volume activity for each scan. A typical contrast **c** is shown above (this is not strictly a contrast because it

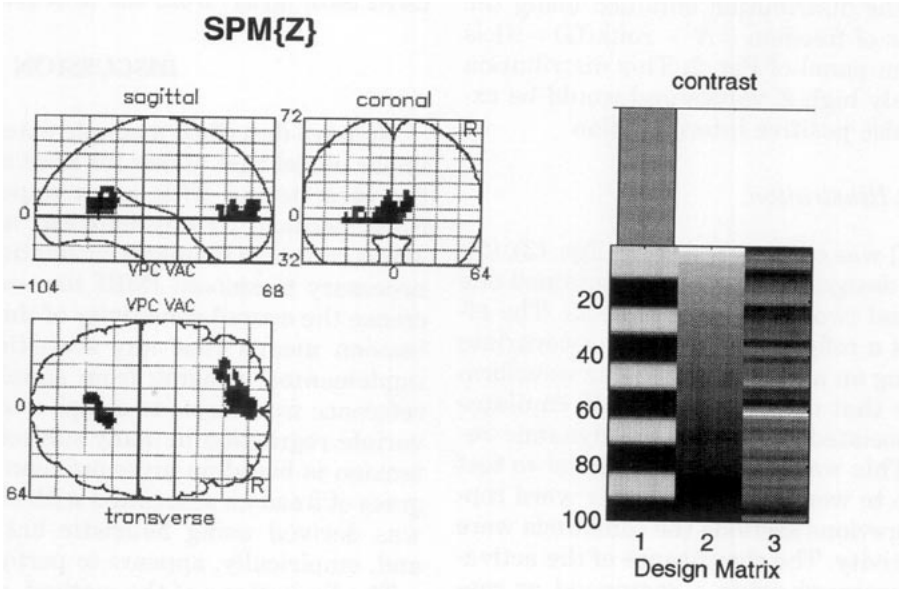

Deactivations

region	size {k}	P(n max > k)	Z	P(Z max > u) (Uncorrected)	{x,y,z mm}
1	**277**	**0.000**	**3.96**	**0.749** (0.000)	**−2 52 8**
			3.81	1.216 (0.000)	−6 42 0
			3.24	6.673 (0.001)	−32 34 0
2	**149**	**0.014**	**3.70**	**1.723** (0.000)	**10 −50 12**
			3.62	2.238 (0.000)	−2 −56 12
			3.40	4.227 (0.000)	−6 −66 12

Threshold = 2.33; Volume [S] = 37912 voxels; df = 41

FWHM = [8.3 8.1 8.9] mm (i.e. 1027 RESELS)

FIG. 4. The same as Fig. 3 but for deactivations due to word generation.

does not sum to zero but it gives a valid compound). This contrast tests for the significance of the regression coefficient of the sixth random covariate. Six such contrasts were specified testing for the effect of each random covariate in turn.

The convolution matrix $\mathbf{K}$ used a Gaussian kernel with parameter $s = \sqrt{8}$ s = $\sqrt{8/3} = 0.94$ scans. Despite the fact we had 100 scans the effective degrees of freedom were only 38.5. The resulting distribution of Z values (after transformation) pooled over the six SPM{Z} is seen in Fig. 2 (top) and concur remarkably well with the expected distribution under the null hypothesis (broken line).

To emphasise the importance of accounting for temporal correlations the distribution obtained using the uncorrected degrees of freedom = N − rank($\mathbf{G}$) = 91 is shown in the bottom panel of Fig. 2. This distribution gives inappropriately high Z values and would be extremely prone to false positive interpretation.

Data Analysis—An Illustration

A volume SPM{Z} was constructed using Eqs. (3), (5), (6), and (10) and a design matrix $\mathbf{G}$ that contained one effect of interest and two confounding effects. The effect of interest was a reference waveform or covariate obtained by delaying an appropriate box-car waveform by two scans (note that convolution with $\mathbf{K}$ emulates the dispersion associated with the hemodynamic response function). This waveform was designed to test for activations due to word generation over word repetition. As in the previous sections the confounds were time and global activity. The significance of the activation effects were assessed using a compound or contrast $\mathbf{c}$ = [1 0 0]. Figure 3 shows the results of this analysis. The design matrix $\mathbf{G}$ is depicted in the top right panel and shows the time-dependent structure of the three effects modeled. The contrast on top is over the reference waveform or covariate tested. The SPM{Z} thresholded at $P = 0.01$ (uncorrected) reveals significant ($P < 0.05$ corrected) activation in the left prefrontal regions, the cingulate cortex and left precuneus. A right prefrontal region is seen that has a corrected P value of 0.07. Foci that failed to reach a corrected P value of 0.1 are not shown. Tabular data on these regional effects are presented in the bottom panel and include the size of each region (k), its corrected significance based on k using Eq. (13), the peak height Z and the corresponding significance based on Eq. (12), the uncorrected P value, and finally the rough location in Talairach coordinates. For each region the three largest maxima are displayed (if there are more than one).

Significant deactivations are shown in Fig. 4 using the same format as in Fig. 3. Deactivations are seen in the medial prefrontal cortex and in the retrosplenial cortex. These regions are considered significant by virtue of their extensive size. The results are very consistent with the known functional anatomy of word generation established with PET (e.g., Frith *et al.*, 1991). Of particular note are the reciprocal changes in activity in the anterior cingulate and posterior cingulate (retrosplenial cortex). This characteristic interaction is often seen in PET studies.

Figure 5 shows the data from a voxel in the cingulate gyrus plotted against (left) and with (right) the reference covariate. These data give an idea of how consistent the response to changing cognition can be. The symmetry of the bifrontal activation is highlighted in Fig. 6 where the SPM{Z} (coloured) has been rendered onto three orthogonal sections through the original fMRI data (gray) from the first scan.

DISCUSSION

We have described a simple extension to the general linear model that allows for known autocorrelations in the error terms. This is an important extension for fMRI because (i) physiological noise in fMRI time-series can show temporal correlations and (ii) it is often necessary to smooth fMRI time-series in order to increase the overall sensitivity of the technique. This extension means that any statistical analysis can be implemented, ranging from simple regressions using reference waveforms to complex interactions or multivariate regression in many subjects or groups. The extension is based on an expression for the effective degrees of freedom associated with error. This expression was derived using heuristic but sensible reasoning and, empirically, appears to perform very well.

The limitations of the method, as described, include the following. The images must be reasonable lattice representations of a Gaussian field. This usually requires the data to be smooth in space with potential constraints on resolution. However, these constraints are only relative in the sense that the data should be smoother than voxel size (we suggest that the effective

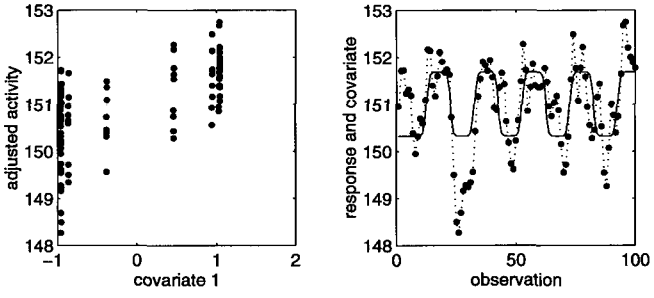

FIG. 5. Plots of the fMRI signal from a voxel in the cingulate gyrus. (Left) Plotted against the reference covariate seen in the design matrix of the previous figures (Figs. 3 and 4). (Right) The same data but plotted as functions of time. The solid line is the reference covariate and the broken line and dots represent the empirical adjusted data $\mathbf{X}^*$.

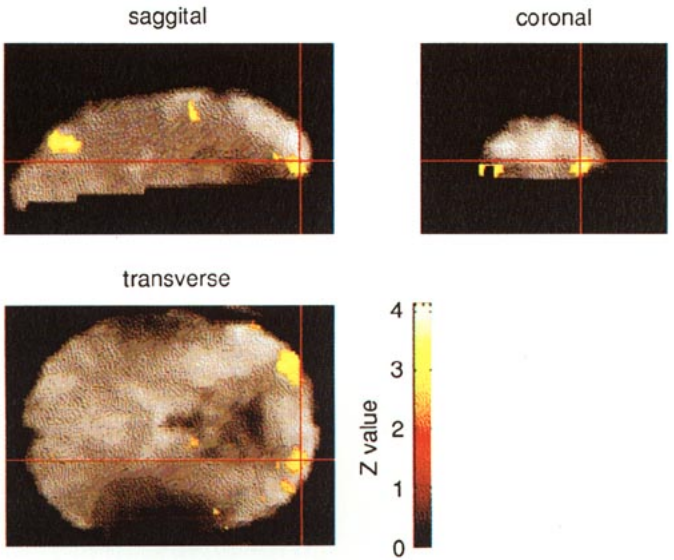

FIG. 6. The SPM{Z} from Fig. 3 has been sectioned and rendered on the fMRI data from the first scan. This display format highlights the functional anatomy of the bifrontal activations.

FWHM be at least twice voxel size), and voxel size is under experimental control. For example these techniques could be applied to MRI microscopy data. Second, for computational expediency, we assume that the physiological autocorrelations do not substantially contribute to the autocorrelations after smoothing. This assumption means that one does not have to estimate smoothness or spectral densities. While this is probably justified for most data (see validation section above) there may be situations where correlations among the error terms are greater than predicted by the smoothing alone. In these situations the effective degrees of freedom can be estimated directly from the residual terms using Eq. (9) or a Gaussian form for the autocorrelation can be assumed and its parameter estimated from the smoothness of the error terms as described in Friston *et al.* (1994a).

CONCLUSION

We hope that this communication facilitates the analysis of fMRI data in a way that provides greater latitude in experimental design and statistical inference.

ACKNOWLEDGMENTS

K.J.F., A.P.H., R.S.J.F., and R.T. are supported by the Wellcome Trust. We thank our colleagues for help and support during the development of these ideas, particularly Keith Worsley. We are grateful to colleagues at the Institute of Psychiatry, Denmark Hill, UK, for essential help in acquiring the data.

REFERENCES

Adler, R. J. 1981. *The Geometry of Random Fields.* Wiley, New York.

Bandettini, P. A. 1993. MRI studies of brain activation: Temporal characteristics. In *Functional MRI of the Brain,* pp. 143–151. Society of Magnetic Resonance in Medicine, Berkeley CA.

Chatfield, C., and Collins, A. J. 1980. *Introduction to Multivariate Analysis,* pp. 189–210. Chapman & Hall, London.

Friston, K. J., Frith, C. D., Liddle, P. F., and Frackowiak, R. S. J. 1991. Comparing functional (PET) images: The assessment of significant change. *J. Cereb. Blood Flow Metab.* **11:**690–699.

Friston, K. J., Jezzard, P., and Turner, R. 1994a. Analysis of functional MRI time-series. *Human Brain Mapping* **2:**69–78.

Friston, K. J., Worsley, K. J., Frackowiak, R. S. J., Mazziotta, J. C., and Evans, A. C. 1994b. Assessing the significance of focal activations using their spatial extent. *Human Brain Mapping* **1:**214–220.

Friston, K. J., Ashburner, J., Poline, J. B., Frith, C. D., Heather, J. D., and Frackowiak, R. S. J. Spatial realignment and normalization of images, submitted for publication.

Frith, C. D., Friston, K. J., Liddle, P. F., and Frackowiak, R. S. J. 1991. Willed action and the prefrontal cortex in man. *Proc. R. Soc. London B* **244:**241–246.

Talairach, J., and Tournoux, P. 1988. *A Co-planar Stereotaxic Atlas of a Human Brain.* Thieme, Stuttgart.

Worsley, K. J., Evans, A. C., Marrett, S., and Neelin, P. 1992. A three-dimensional statistical analysis for rCBF activation studies in human brain. *J. Cereb. Blood Flow Metab.* **12:**900–918.

Worsley, K. J. 1994. Local maxima and the expected Euler characteristic of excursion sets of χ^2, F and t fields. *Adv. Appl. Prob.* **26:**13–42.